

## Nanoscale radio-frequency thermometry

D. R. Schmidt, C. S. Yung, and A. N. Cleland

*Department of Physics, University of California, Santa Barbara, California 93106*

(Received 21 March 2003; accepted 22 May 2003)

We experimentally demonstrate the high bandwidth readout of a thermometer based on a superconductor–insulator–normal metal (SIN) tunnel junction, embedded in a rf resonant circuit. Our implementation enables basic studies of the thermodynamics of mesoscopic nanostructures. It can also be applied to the development of fast calorimeters, as well as ultrasensitive bolometers for the detection of far-infrared radiation. We discuss the operational details of this device, and estimate the ultimate temperature sensitivity and measurement bandwidth. © 2003 American Institute of Physics. [DOI: 10.1063/1.1597983]

Thermodynamic studies of mesoscopic devices have lagged far behind the corresponding electrical and magnetic investigations. This dearth can be attributed to a lack of fast, robust thermometers that can be easily integrated with nanoscale structures. Electronic thermometers that function at very low temperatures and have fast response times will enable future probes of thermal physics at smaller size scales and shorter time spans than have previously been explored, and are also a key technology for far-infrared bolometry. In this letter, we describe our development of a nanoscale thermometer, based on a superconductor–insulator–normal metal (SIN) tunnel junction, that should allow thermodynamic measurements in the 1–100-MHz frequency range.

The measurement of temperature in nanoscale systems is a difficult problem for which a number of different approaches have been used. One very sensitive technique is to use a dc superconducting quantum interference device to measure the Johnson–Nyquist noise in a normal metal film. This approach has been used to measure electron–phonon coupling effects in normal metal films,<sup>1,2</sup> as well as in the first observation of the quantum of thermal conductance for phonons<sup>3</sup> by Schwab and coworkers.<sup>4</sup> By contrast, the earlier measurement of the quantum of thermal conductance for electrons<sup>5,6</sup> used the thermoelectric effect in a quantum point contact. Another semiconductor-based method uses the temperature dependence of weak localization in heavily doped GaAs.<sup>7</sup> Thermopower in mesoscopic AuFe wires has been extensively studied using noise thermometry with conventional amplifiers.<sup>8</sup>

Here, we describe the use of submicron SIN tunnel junctions as high-speed thermometers. Large-area SIN tunnel junctions have been used as the thermistor element in bolometric applications,<sup>9</sup> and we have previously used mechanically-suspended SIN junctions as low-frequency thermometers to confirm the measurement of the quantum of thermal conductance.<sup>10</sup> At temperatures sufficiently below the superconducting transition temperature  $T_C$ , the tunnel junction's small-signal resistance at zero bias,  $R_0 \equiv dV/dI(0)$ , is exponentially dependent on the ratio of temperature  $T$  to the superconducting energy gap  $\Delta$ ,  $R_0 \propto e^{\Delta/k_B T}$ . This resistance can be measured using very small bias currents, with negligible self-heating. The resulting high responsivity of the SIN junction, and the fact that it can be

well impedance-matched to room-temperature amplifiers, allows its use in a variety of situations. For example, full density-of-states measurements have been made on mesoscopic devices with SIN junctions.<sup>11</sup>

Previous applications of submicron SIN tunnel-junction thermometers have been conducted under dc or audio-frequency heating conditions. However, these tunnel junctions should be able to operate at much higher frequencies. The intrinsic electrical bandwidth is set by the product of the tunnel resistance  $R_0$  and the junction capacitance  $C_J$ ,  $f_{3\text{ dB}} = 1/2\pi R_0 C_J$ . For a fixed tunnel barrier thickness, this product is independent of the junction area  $A$ . With typical values of  $R_0 A \sim 10^3 \Omega \mu\text{m}^2$  and  $C_J/A \sim 10^{-13} \text{ F}/\mu\text{m}^2$ , this corresponds to  $f_{3\text{ dB}} \sim 2 \text{ GHz}$ .

The time scale for the thermal relaxation of the normal metal electrons depends on the cooling mechanism. Diffusive cooling of the electrons into a larger normal metal volume occurs at time scales dictated by the diffusion constant, and can be made less than 1 ns. The time scale for cooling via phonon emission is set at low temperatures by the electron–phonon relaxation time, and possibly by the quasi-particle relaxation time in the superconductor. The small-signal electron–phonon thermal conductance to the substrate is  $G_{e-p} = 5\Sigma VT^4$ , where  $\Sigma$  is a material-dependent parameter and  $V$  the normal metal volume.<sup>2,12</sup> The electronic heat capacity is also proportional to volume,  $C_e = \gamma VT$ , resulting in a volume-independent thermal time constant  $\tau_{\text{th}} = C/G_{e-p} = \gamma/5\Sigma T^3 \sim 10 T^{-3} \text{ ns K}^3$ .<sup>13</sup> The relaxation rate of a phonon-cooled metal is thus about  $1/\tau_{\text{th}} \sim 10^8 \text{ Hz}$  at 1 K, and  $10^5 \text{ Hz}$  at 100 mK.

Stray cabling capacitance limits the measurement bandwidth of many mesoscopic devices to the audio range. A number of researchers have recognized the merits of using rf resonant circuits to eliminate the bandwidth-reducing effect of this capacitance. The device is placed in a resonant circuit with a discrete inductor  $L$  and capacitance  $C$ , such that the device resistance acts to damp the circuit resonance (see Fig. 1). Thus, the resistance measurement can be performed by measuring the power reflected from the  $LC$  circuit near its resonance frequency  $f_{\text{res}} = 1/2\pi\sqrt{LC}$ , which can easily be arranged to fall in the 50–2000-MHz range. Gödel *et al.*<sup>14</sup> employed this technique to measure a quantum point contact.

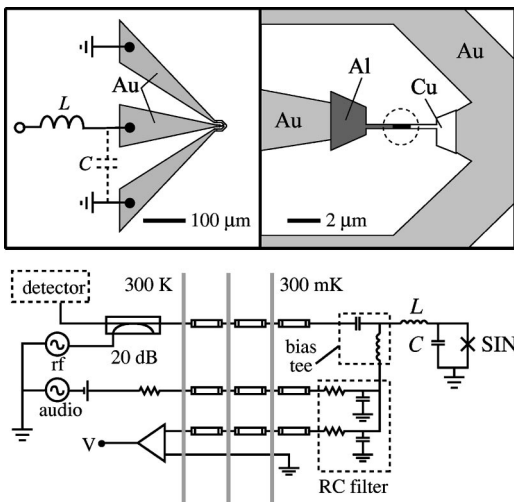


FIG. 1. Top: Schematic of the tunnel-junction layout, on the right showing the metal electrode geometry with the tunnel junction in the dotted circle, and on the left the larger-scale bond pads with the  $LC$  circuit, the  $C$  due to the capacitance of the bond pads. Bottom: Readout circuit, configured for simultaneous dc and rf measurements. All electrical leads are thermally clamped at each stage of the cryostat, and the dc and rf portions are connected together through a rf bias tee. The resonant circuit comprises the inductor  $L$  and capacitance  $C$ , the latter in parallel with the tunnel junction SIN.

Record charge sensitivity was achieved by Schoelkopf *et al.*<sup>15</sup> by reading out a single-electron transistor (SET) in a  $LC$  resonant circuit. Fujisawa *et al.*<sup>16</sup> used a qualitatively similar transmission-based measurement to study the high-frequency noise in a GaAs quantum dot. The maximum readout bandwidth  $\Delta f$  is set by the width of the  $LC$  resonance, which for a large resistance device is set by the  $Z_0 = 50 \Omega$  cable, and is of order  $\Delta f = f_{\text{res}}/Q = Z_0/2\pi L \sim 10 - 100$  MHz. While a frequency of 100 MHz is still below the intrinsic electrical bandwidth of the SIN junction, it is sufficient to allow the measurement of the electron-phonon relaxation time for a submicron SIN thermometer as well as other phonon-mediated relaxation processes.

We fabricated the SIN tunnel junctions using a standard multiple-angle evaporation technique, using Cu as the normal metal and Al as the superconductor.<sup>17</sup> The tunnel junction had a 90 nm thick Al layer and a 90 nm thick Cu layer, with an overlap area of  $0.3 \times 1.0 \mu\text{m}^2$ , and a normal state resistance of 2.5 k $\Omega$ . The Cu normal metal element is electrically and thermally connected to the Au ground lead.

We glued the GaAs chip to a printed circuit board mounted in a small metal box, and made electrical connections using Au wire bonds. A surface-mounted coil provided  $L = 390$  nH of inductance. The stray resonant capacitance  $C = 0.6$  pF resulted in a  $LC$  resonance frequency of about  $f_{\text{res}} = 340$  MHz.

The box containing the SIN junction was mounted in a  $^3\text{He}$  cryostat wired with the measurement circuit shown in Fig. 1. The current-voltage characteristics for temperatures from 310 to 950 mK are shown in Fig. 2, with the differential resistance at 315 mK shown in inset (a). The measured superconducting voltage gap is  $2\Delta/e = 386 \mu\text{V}$ , typical for thin film Al. The differential resistance at zero bias  $R_0(T)$  is plotted in inset (b).

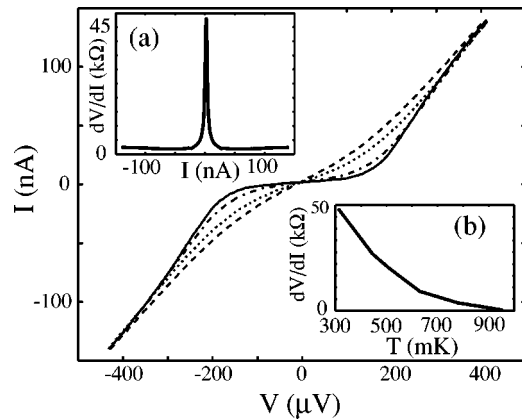


FIG. 2. Dc current-voltage characteristics, measured at a number of different temperatures. The superconducting gap of Al is easily visible at the lowest temperature (solid line: 315 mK) which was thermally smeared as the temperature was raised (dash-dot, 510 mK; dotted, 780 mK; dashed, 950 mK). Inset (a): Bias-dependent differential resistance  $R(I) = dV/dI(I)$  at 315 mK. Inset (b): Zero-bias resistance  $R_0$  as a function of temperature.

We then measured the reflected rf power from the  $LC$  resonator with the embedded tunnel junction. For swept frequency measurements, an rf signal was generated at the source (reflection) port of a two-port network analyzer, and used to measure the reflection coefficient of the resonator as a function of both dc current bias and temperature. The source power at the top of the cryostat was typically  $-100$  dBm (100 fW), with a one-way cable loss of about 2.5 dB. We display our measurements in terms of the total round-trip return loss  $R_{\text{loss}}$ , including the cable loss.

Figure 3(a) shows the measured return loss at the  $LC$  resonance frequency, as a function of dc current bias. The return loss is given by  $R_{\text{loss}} = |(Z_0 + Z)/(Z_0 - Z)|^2$ , where  $Z$  is the  $LC$  resonator impedance,  $Z \approx R/Q^2$  for an SIN differential resistance  $R = dV/dI$  measured on resonance. The return loss clearly corresponds to the dc differential resistance shown in Fig. 2(a). Below 510 mK, additional structure appears, as shown in Fig. 3(b). This double-lobed behavior is easily understood: For one value of  $R$ , the  $LC$  resonant circuit is most closely matched to the cable impedance  $Z_0$ , maximizing the return loss at that point. This occurs for  $R(I) = 22$  k $\Omega$  in our measurements. This is also exhibited in the temperature dependence of the return loss, shown in Fig. 4(a). The maximum in the return loss is observed at  $\sim 510$  mK, for which  $R_0 = dV/dI(I=0) \sim 20$  k $\Omega$ . The optimal temperature range for rf thermometry can be controlled by the choice of circuit parameters.

Finally, we measured the noise properties of the rf thermometer, using a mixer to detect the reflected power. The mixer local oscillator (LO) was provided by a separate signal source phase-locked to the rf drive. The phase of the LO was adjusted to achieve monotonic response as a function of bias. The mixer output was low-pass filtered ( $< 20$  MHz), amplified and Fourier transformed using a dynamic signal analyzer, allowing measurement of the noise from dc to 100 kHz.

The dominant source of noise was from the first-stage amplifier, and as expected was flat, with no measurable  $1/f$  component. For an input power of  $-110$  dBm (10 fW) to the  $LC$  resonator, we measured a resistance noise of  $40 \Omega/\text{Hz}^{1/2}$ .

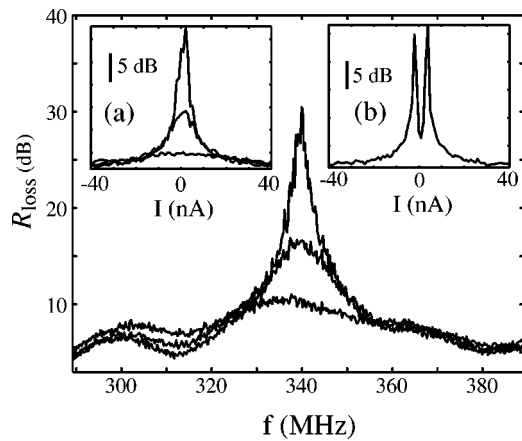


FIG. 3. Return loss as a function of drive frequency. The  $LC$  resonance is strongly modulated by biasing the SIN junction, shown by the three curves at 0.0, 6.0, and 13.0 nA. The return loss  $R_{\text{loss}}$  includes the contribution due to the cable. Higher  $R_{\text{loss}}$  indicates lower reflected power. Inset (a) Bias-dependent return loss at 338.92 MHz for 510, 630, and 950 mK. The peak in  $R_{\text{loss}}$  is suppressed at 950 mK. The analogous dc measurement is shown in Fig. 2(a). Inset (b) At 315 mK the return loss at 338.92 MHz is doubly-peaked as a function of current bias.

Using a temperature responsivity  $dT/dR$  of  $7 \mu\text{K}/\Omega$ , we calculate the temperature noise to be  $\sim 280 \mu\text{K}/\text{Hz}^{1/2}$ . While this is comparable to the spectral noise density of the dc measurement for similar input power, the bandwidth is far higher.

This noise figure is very promising for our measurement system, but leaves significant room for improvement. The first-stage amplifier can be operated at cryogenic temperatures, improving its input noise by a factor of 15. Secondly, lowering the temperature of the SIN tunnel junction to below 300 mK would increase the sensitivity. Lastly, the input rf power and frequency can be optimized for largest signal. These contributions are multiplicative, and each can realistically lower the noise by about an order of magnitude. We therefore estimate that a noise temperature of better than  $1 \mu\text{K}/\text{Hz}^{1/2}$  is attainable. The measurement bandwidth achieved using our resonant circuit is approximately the width of the resonance shown in Fig. 3, or about 10 MHz. If an optimized SIN-based thermometer were integrated into a bolometer, it would potentially be able to detect single few-THz photons at count rates of up to about  $10^7$  Hz.<sup>18</sup>

In conclusion, we have demonstrated a technique to measure the temperature of the normal metal side of an SIN tunnel junction thermometer with a bandwidths of up to 100 MHz. This rf-SIN opens up possibilities for studies of basic thermodynamics in nanostructures, and for bolometric detector technology. Thermodynamic measurements can now be performed at sub- $\mu\text{s}$  time scales with the rf-SIN.

We acknowledge financial support provided by the

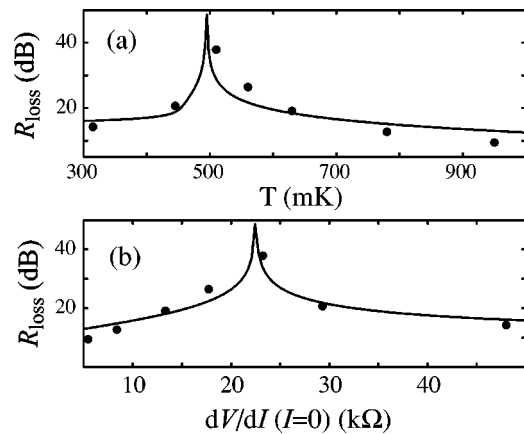


FIG. 4. (a) Temperature dependence of the return loss at zero bias and 338.92 MHz is nonmonotonic and peaked at  $\sim 510$  mK. (b) The data shown in (a) and from Fig. 2(b) were used to extract the dependence of return loss on the differential resistance of the tunnel junction. When the  $dV/dI(0) \sim 22 \text{ k}\Omega$ , the resonator is closely matched to the cable impedance and the return loss is maximized. In (a) and (b), the solid line is a calculated result, assuming optimal matching to the cable impedance at  $dV/dI \sim 22 \text{ k}\Omega$ .

NASA Office of Space Science under grant NAG5-11426, the Army Research Office under Award DAAD-19-99-1-0226.

- <sup>1</sup>M. L. Roukes, M. R. Freeman, R. S. Germain, R. C. Richardson, and M. B. Ketchen, *Phys. Rev. Lett.* **55**, 422 (1985).
- <sup>2</sup>F. C. Wellstood, C. Urbina, and J. Clarke, *Phys. Rev. B* **49**, 5942 (1994).
- <sup>3</sup>L. G. C. Rego and G. Kirzenow, *Phys. Rev. Lett.* **81**, 232 (1998).
- <sup>4</sup>K. Schwab, E. A. Henriksen, J. M. Worlock, and M. L. Roukes, *Nature (London)* **404**, 974 (2000).
- <sup>5</sup>L. W. Molenkamp, T. Gravier, H. van Houten, O. J. A. Buijk, M. A. A. Mabesoone, and C. T. Foxon, *Phys. Rev. Lett.* **68**, 3765 (1992).
- <sup>6</sup>A. Greiner, L. Reggiani, T. Kuhn, and L. Varani, *Phys. Rev. Lett.* **78**, 1114 (1997).
- <sup>7</sup>T. S. Tighe, J. M. Worlock, and M. L. Roukes, *Appl. Phys. Lett.* **70**, 2687 (1997).
- <sup>8</sup>C. Strunk, M. Henny, C. Schönenberger, G. Neuttiens, and C. V. Haesendonck, *Phys. Rev. Lett.* **81**, 2982 (1998).
- <sup>9</sup>M. Nahum and J. M. Martinis, *Appl. Phys. Lett.* **63**, 3075 (1993).
- <sup>10</sup>C. S. Yung, D. R. Schmidt, and A. N. Cleland, *Appl. Phys. Lett.* **81**, 31 (2002).
- <sup>11</sup>H. Pothier, S. Guéron, N. O. Birge, D. Esteve, and M. H. Devoret, *Phys. Rev. Lett.* **79**, 3490 (1997).
- <sup>12</sup>V. F. Gantmakher, *Rep. Prog. Phys.* **37**, 317 (1974).
- <sup>13</sup>See Ref. 10: Yung *et al.* determined that  $\Sigma \sim 2 \times 10^{-9} \text{ W}/(\mu\text{m}^3 \text{ K}^5)$ . At low temperatures,  $\gamma \sim 10^{-16} \text{ J}/(\mu\text{m}^3 \text{ K}^2)$  for Cu.
- <sup>14</sup>W. Gödel, S. Manus, D. Wharam, J. P. Kotthaus, G. Böhm, W. Klein, G. Tränkle, and G. Weimann, *Electron. Lett.* **30**, 977 (1994).
- <sup>15</sup>R. J. Schoelkopf, P. Wahlgren, A. A. Kozhevnikov, P. Delsing, and D. E. Prober, *Science* **280**, 1238 (1998).
- <sup>16</sup>T. Fujisawa and Y. Hirayama, *Appl. Phys. Lett.* **77**, 543 (2000).
- <sup>17</sup>T. A. Fulton and G. J. Dolan, *Phys. Rev. Lett.* **59**, 109 (1987).
- <sup>18</sup>A  $0.005\text{-}\mu\text{m}^3$  Cu normal metal element has a heat capacity  $C \sim 1 \times 10^{-19} \text{ J/K}$  at 200 mK. A 5-THz photon then raises the temperature by  $\sim 30$  mK. For a noise figure of  $1 \mu\text{K}/\text{Hz}^{1/2}$  and 10-MHz bandwidth, the single photon signal would equal the rms temperature noise.